

Current noise of a resonant tunnel junction coupled to a nanomechanical oscillator

M. Tahir* and A. MacKinnon†

*The Blackett Laboratory, Imperial College London,
South Kensington campus, London SW7 2AZ, United Kingdom*

We present a theoretical study of current noise of a resonant tunnel junction coupled to a nanomechanical oscillator within the non-equilibrium Green's function technique. An arbitrary voltage is applied to the tunnel junction and electrons in the leads are considered to be at zero temperature. The properties of the phonon distribution of the nanomechanical oscillator strongly coupled to the electrons on the dot are investigated using a non-perturbative approach. Analytical calculations and numerical results for the current-voltage, shot noise and the corresponding Fano factor as a function of applied bias show significant features of the nanomechanical oscillator coupling dynamics. This will provide useful insight for the design of experiments aimed at studying the quantum behavior of an oscillator.

PACS numbers: 73.23.Hk, 85.85.+j

I. INTRODUCTION

In recent years, there has been a great interest in the measurement of current noise near the quantum limit of displacement sensitivity using single electron transistors (SET) and nanomechanical oscillators¹⁻⁶. Current noise is the non-equilibrium fluctuation which is caused by the discreteness of charged carriers. When the size of an electromechanical system reaches the nanometer scale, the current noise problem becomes a very interesting aspect of the NEMS⁷⁻¹⁰ based devices. In NEMS devices it is a fundamental physical signature, which can provide us additional information regarding quantum transport, in addition to differential conductance and current voltage characteristics. The electrons traveling through the device become correlated in the same channel and the same probe, as well as in different channels and different probes. For a mesoscopic system, the electrons are correlated due to coherent transport and they are governed by the Fermi distribution and Coulomb blockade. Noise is caused by the randomness of electron scattering and it has been extensively studied in different types of mesoscopic structures. For uncorrelated electrons travelling through a macroscopic conductor, shot noise $S(0)$ at zero frequency is given by the Poisson value $S(0) = 2eI$, where I is the net average current flowing through the system. However, for a mesoscopic system, electrical current correlations are dominated by the Coulomb blockade and a Fermi distribution can lead to the deviation of shot noise from a Poissonian ($F=1$) form. An important parameter for describing this type of shot noise is the Fano factor $F = S(0)/2eI$, using which the shot noise can be classified as sub-Poissonian ($F < 1$) or super-Poissonian ($F > 1$). Similarly, phonon assisted features have been observed in molecular systems¹¹⁻¹⁴ with strong interactions, which is beyond the scope of perturbation theory.

In general, there are two different theoretical formulations that can be used to study the quantum transport in nanoscopic systems under voltage bias. Firstly, a generalized quantum master equation approach¹⁵⁻²⁰ and secondly, the non-equilibrium Green's function formula-

tion²¹⁻²⁵. The former leads to a simple rate equation, where the coupling between the dot and the leads is considered as a weak perturbation and the electron-phonon interaction is also considered very weak. In the latter case one can consider strong leads to system and electron-phonon coupling. The non-equilibrium Green's function technique is able to deal with a very broad variety of physical situations related to quantum transport at molecular²⁶⁻²⁸ levels. It can deal with strong non-equilibrium situations and very small to very large applied bias. In most of the theoretical work on NEMS devices, the mechanical degree of freedom has been described classically/semiclassically^{15,16} using the master equation approach or quantum mechanically^{17-20,34,35} using the perturbation approach for the electron-phonon interactions. Furthermore, Shot noise for electron transport in molecular devices was investigated within a scattering theory approach^{29,30}. Phonon effects in the noise spectrum were studied recently³¹⁻³³, in connection with NEMS and both single electronic levels in quantum dots and single molecules. In Armour's work¹⁵, the mechanical part was also treated classically, including the damped oscillator and assuming a weak electron tunneling process. This approach is based on a perturbation, weak coupling and large applied bias approximations, whereas the Keldysh non-equilibrium Green's function formulation can treat the system-leads and electron-phonon coupling with strong interactions for both small and large applied bias voltage. Moreover, these theories fail to explain the low bias regime. The transport properties have been described and discussed semiclassically/classically but need a complete quantum mechanical description. A theory beyond these cases is required to further refine experiments to investigate the quantum transport properties of NEMS devices.

In the present work, we employ the non-equilibrium Green's function method to discuss the current-voltage and shot noise properties of a NEMS device. This is a fully quantum mechanical formulation whose basic approximations are very transparent, as the technique has already been used to study transport properties in a wide

range of systems. The main differences between existing work and ours are: in most of the existing literature a very large chemical potential difference is considered while we are able to include a range from very small to very large. In our calculation the inclusion of the oscillator is not perturbative as the STS experiments^{11–14} are beyond the range of perturbation theory. Hence, an approach is required beyond the quantum master equation or linear response. Hence, our work provides an exact analytical solution to the current–voltage, shot noise, coupling of leads with the system, very small to very large chemical potential difference and includes both the right and left Fermi level response regimes. For simplicity, we used the wide–band approximation, where the coupling between the leads and the dot is taken to be independent of energy. This provides a way to perform transient transport calculations from first principles while retaining the essential physics of the electronic structure of the dot and the leads. Another advantage of this method is that it treats the infinitely extended reservoirs in an exact way in the present system, which may give a better understanding of the essential features of NEMS in a more appropriate quantum mechanical picture.

II. MODEL CALCULATIONS

We consider a single quantum dot connected to two identical metallic leads via tunnel junctions (SET device)^{15,19,35}. A single nanomechanical oscillator is coupled to the electrons on the dot and the applied gate voltage is used to tune the single level of the dot. This model represents a close analog of an electromechanical displacement detector and contains the essential features of the recent experiments performed with a resonator^{1,2}, or a vibrating beam of crystal or cantilever coupled to the SET device^{3–6}. In most of these experiments, the motion of a resonator (nanomechanical oscillator) may be detected by capacitively coupled electrodes placed on the resonator and biasing the electrode at a constant voltage. The dot has a small capacitance due to its small diameter (nm) and thus has charging energy. This charging energy exceeds the thermal energy in these experiments. For this reason we consider that only one excess electron may occupy the device. To ensure this condition we are working at zero temperature.

In the present simple model, both the electronic and the mechanical degrees of freedom have been treated quantum mechanically, where the nanomechanical oscillator is represented in terms of creation and annihilation operators. We neglect the spin degree of freedom and electron–electron interaction effects and consider the simplest possible model system. We also neglect the effects of finite electron temperature of the lead reservoirs and damping of the oscillator. Our model consists of the individual entities such as the single quantum dot with perpendicular oscillator on it and the left and right leads in their ground states at zero temperature. The Hamil-

tonian of our simple system^{24–26,28} is

$$H_0 = H_{ph-dot} + H_{leads} \quad (1)$$

$$H_{dot-ph} = [\epsilon_0 + \eta(b^\dagger + b)] c_0^\dagger c_0 + H_{ph}, \quad (2)$$

$$H_{ph} = \frac{\hat{p}^2}{2\mu} + \frac{1}{2}\mu\omega^2\hat{x}^2 = \hbar\omega(b^\dagger b + \frac{1}{2}), \quad (3)$$

where ϵ_0 is the single energy level of electrons on the dot with c_0^\dagger, c_0 the corresponding creation and annihilation operators. The parameter $\eta = \lambda l / \sqrt{2}$ physically represents an effective electric field in the capacitor formed by the oscillator and the dot electrons, which we shall call coupling strength between the oscillator and the electrons on the dot given as $\lambda l = eEl$, where e is the charge of electron, E is the strength of the electric field and $l = \sqrt{\frac{\hbar}{\mu\omega}}$ is the zero point amplitude of the oscillator with mass μ . Here we assume that the energy of the resonant level depends linearly on the oscillator coordinate. The frequency of the nanomechanical oscillator is ω and b^\dagger, b are the raising and lowering operator of the phonons given as

$$\hat{x} = \frac{l}{\sqrt{2}}(b^\dagger + b), \quad (4)$$

and

$$\hat{p} = \frac{i\mu\omega}{\sqrt{2}}l(b^\dagger - b), \quad (5)$$

The remaining elements of the Hamiltonian are

$$H_{leads} = \sum_j \epsilon_j c_j^\dagger c_j, \quad (6)$$

$$\Delta H_\alpha = H_{leads-dot} = \frac{1}{\sqrt{N}} \sum_j V_\alpha (c_j^\dagger c_0 + c_0^\dagger c_j), \quad (7)$$

where N is the total number of states in the lead, V_α is the hopping between the dot and the leads $\alpha = L, R$, j represents the channels in one of the leads. For the second lead the Hamiltonian can be written in the same way.

The total Hamiltonian of the system is thus $H = H_0 + \Delta H_\alpha$. We write the eigenvalues and the eigenfunctions of H_{dot-ph} as

$$\epsilon = \epsilon_0 + \hbar\omega(n + \frac{1}{2}) - \Delta \quad (8)$$

$$\Psi_n(K, x_0 = 0) = A_n \exp[-\frac{l^2 K^2}{2}] H_n(lK), \quad (9)$$

$$\Psi_n(K, x_0 \neq 0) = \Psi_n(K, x_0 = 0) \exp[-iKx_0] \quad (10)$$

for the occupied, $x_0 \neq 0$ and unoccupied, $x_0 = 0$, dot respectively, where $A_n = 1/\sqrt{\pi 2^n n! l}$, $\Delta = \lambda^2 / \mu\omega^2$. $x_0 = \lambda / \mu\omega^2$ is the shift of the oscillator due to the coupling to the electrons on the dot and $H_n(lK)$ are the

usual Hermite polynomials. Here we have used the fact that the harmonic oscillator eigenfunctions have the same form in both real and Fourier space.

In order to transform between the representations for the occupied and unoccupied dot we require the matrix with elements

$$\Phi_{n,m} = \int \Psi_n^*(K, x_0 = 0) \Psi_m(K, x_0 \neq 0) dK, \quad (11)$$

which may be simplified³⁶ as

$$\Phi_{n,m} = \sqrt{\frac{2^{m-n} n!}{m!}} \exp\left(-\frac{1}{4}x^2\right) \left(\frac{1}{2}ix\right)^{m-n} L_n^{m-n}\left(\frac{1}{2}x^2\right) \quad (12)$$

for $n \leq m$, where $x = \frac{x_0}{l}$ and $L_n^{m-n}(x)$ are the associated Laguerre polynomials. Note that the integrand is symmetric in m and n but the integral is only valid for $n \leq m$. Clearly the result for $n > m$ is obtained by exchanging m and n in equation (12) to obtain

$$\Phi_{n,m} = \sqrt{\frac{2^{|m-n|} \min[n,m]!}{\max[n,m]!}} \exp\left(-\frac{1}{4}x^2\right) \times \left(\frac{1}{2}ix\right)^{|m-n|} L_{\min[n,m]}^{|m-n|}\left(\frac{1}{2}x^2\right). \quad (13)$$

The position of the resonant level with respect to the chemical potential in the leads is thus affected by the displacement of the nanomechanical oscillator, which in turn affects the transport properties of the junction through the device.

The particle current I_α into the interacting region from the lead is related to the expectation value of the current operator $I_\alpha = \text{Tr}(\rho \hat{J}_\alpha)^{37-40}$, where

$$\hat{J}_\alpha = \frac{ie}{\hbar} \sum_j \{V_{0,\alpha} c_0^\dagger c_{\alpha j} - c_{\alpha j}^\dagger c_0 V_{0,\alpha}\}, \quad (14)$$

$\rho = -iG^<$ and ρ is the density matrix written in terms of the lesser Green's function. Eq. (14) can be written in terms of lesser Green's function as

$$I_\alpha(t) = \frac{e}{\hbar} \{G_{0,\alpha}^<(t,t) V_{\alpha,0}(t) - V_{0,\alpha}^*(t) G_{\alpha,0}^<(t,t)\}, \quad (15)$$

where we have the following relations

$$G_{\alpha,\alpha}^<(t,t) = \int dt' \{G_{0,0}^r(t,t') V_{0,\alpha}(t') g_{\alpha,\alpha}^<(t',t) + G_{0,0}^<(t,t') V_{0,\alpha}(t') g_{\alpha,\alpha}^a(t',t)\} \quad (16)$$

and

$$G_{\alpha,0}^<(t,t) = \int dt' \{g_{\alpha,\alpha}^r(t,t') V_{\alpha,0}(t') G_{0,0}^<(t',t) + g_{\alpha,\alpha}^<(t,t') V_{\alpha,0}(t') G_{0,0}^a(t',t)\}, \quad (17)$$

where $g_{\alpha,\alpha}^{r,(a),(<)}(t,t')$ refers to the unperturbed states of the leads.

$$I_\alpha(t) = \frac{e}{\hbar} \int \text{Tr} \{ (G_{0,0}^r(t,t') V_{0,\alpha}(t') g_{\alpha,\alpha}^<(t',t) + G_{0,0}^<(t,t') V_{0,\alpha}(t') g_{\alpha,\alpha}^a(t',t)) V_{\alpha,0}(t) - V_{0,\alpha}^*(g_{\alpha,\alpha}^r(t,t') V_{\alpha,0}(t') G_{0,0}^<(t',t) + g_{\alpha,\alpha}^<(t,t') V_{\alpha,0}(t') G_{0,0}^a(t',t)) \} dt'. \quad (18)$$

Using the fact that

$$\Sigma_{0,0,\alpha}^{r,(a),(<)}(t',t) = V_{0,\alpha}^*(t') g_{\alpha,\alpha}^{r,(a),(<)}(t',t) V_{\alpha,0}(t),$$

we can simplify the above equation as

$$I_\alpha(t) = \frac{e}{\hbar} \int \text{Tr} \{ G_{0,0}^r(t,t') \Sigma_{0,0,\alpha}^<(t',t) + G_{0,0}^<(t,t') \Sigma_{0,0,\alpha}^a(t',t) - \Sigma_{0,0,\alpha}^r(t,t') G_{0,0}^<(t',t) - \Sigma_{0,0,\alpha}^<(t,t') G_{0,0}^a(t',t) \} dt'. \quad (19)$$

In the stationary regime all of the Green's functions depend on time order $(t - t')$, yielding the Fourier/Laplace transform of equation (19) as

$$I_\alpha = \frac{e}{\hbar} \int \frac{dE}{2\pi} \text{Tr} \{ G_{0,0}^r(E) \Sigma_{0,0,\alpha}^<(E) + G_{0,0}^<(E) \Sigma_{0,0,\alpha}^a(E) - \Sigma_{0,0,\alpha}^r(E) G_{0,0}^<(E) - \Sigma_{0,0,\alpha}^<(E) G_{0,0}^a(E) \}, \quad (20)$$

In order to calculate the analytical results and to dis-

cuss the numerical quantum dynamics of the nanome-

chanical system, our focus is firstly to derive an analytical relation for the retarded self-energy. The self-energy represents the contribution to the dot energy, due to interactions between the dot and the leads. In obtaining these results we use the wide-band approximation where the retarded self-energy of the dot due to each lead is considered to be energy independent and is given by

$$\Sigma_{n_0, n_0, \alpha}^r(E) = \Delta H_{\alpha}^* g_{\alpha, \alpha}^r(E - (n_0 + \frac{1}{2})\hbar\omega) \Delta H_{\alpha}, \quad (21)$$

where off-diagonal element of matrix, $\Sigma_{n_0, n'_0, \alpha}^r(E)$, are zero and $g_{\alpha, \alpha}^r(E - (n_0 + \frac{1}{2})\hbar\omega)$ is the uncoupled Green's function in the leads as

$$\begin{aligned} g_{\alpha, \alpha}^r(E - (n_0 + \frac{1}{2})\hbar\omega) &= \frac{1}{N} \sum_j g_{\alpha, j}^r(E - (n_0 + \frac{1}{2})\hbar\omega) \\ &= \frac{1}{N} \int_{-\infty}^{+\infty} \frac{N n_{\alpha} d\varepsilon_{\alpha}}{E - (n_0 + \frac{1}{2})\hbar\omega - \varepsilon_{\alpha}} \end{aligned} \quad (22)$$

where $\sum_j \mapsto \int_{-\infty}^{+\infty} N n_{\alpha} d\varepsilon_{\alpha}$, j stands for every channel in each lead and n_{α} is the density of states in lead α . With the help of equation (22), the retarded self-energy may be written as

$$\begin{aligned} \Sigma_{n_0, n_0, \alpha}^r(E) &= \Delta H_{0\alpha} \frac{1}{N} \int_{-\infty}^{+\infty} \frac{N n_{\alpha} d\varepsilon_{\alpha}}{E - (n_0 + \frac{1}{2})\hbar\omega - \varepsilon_{\alpha}} \Delta H_{\alpha 0} \\ &= -|V_{0, \alpha}|^2 n_{\alpha} \times (\pi i) = \frac{-i\Gamma_{\alpha}}{2} \end{aligned} \quad (23)$$

which is now independent of E , $\Gamma_{\alpha} = 2\pi |V_{0, \alpha}|^2 n_{\alpha}$, α representing the L or R leads and the retarded self energy is now independent of the oscillator's index (n_0, n_0). Hence, it can be written as $\Sigma_{n_0 n_0, \alpha}^r(E) = (\Sigma_{n_0, n_0, \alpha}^a(E))^* = -\frac{i\Gamma_{\alpha}}{2}$.

We solve Dyson's equation using $H_{dot-lead}$ as a perturbation. For the more general systems we aim to treat in the future, this is a reasonable small parameter. In the present case, however, we can find an exact solution. The retarded and advanced Green's functions on the dot, with the phonon states in the representation of the unoccupied dot, may be written as

$$G_{nn_0}^{r(a)}(E) = \sum_m \Phi_{n, m} g_m^{r(a)}(E) \Phi_{n_0, m}^*, \quad (24)$$

where $g_m^{r(a)}(E)$ is the retarded (advanced) Green's function on the occupied dot,

$$g_m^{r(a)}(E) = [E - \epsilon_0 - (m + \frac{1}{2})\hbar\omega + \Delta \pm i\Gamma]^{-1}, \quad (25)$$

assuming that $\Gamma_L = \Gamma_R = \Gamma$.

The lesser Green's function in the presence of the nanomechanical oscillator including the dot and the leads is written as

$$G_{n, n'}^<(E) = \sum_{n_0, n'_0} G_{n, n_0}^r(E) \Sigma_{n_0 n'_0}^<(E) G_{n'_0, n'}^a(E), \quad (26)$$

with $\Sigma_{n_0, n'_0}^<(E)$ being the the lesser self energy which is given as

$$\Sigma_{n_0, n'_0}^<(E) = \Sigma_{n_0, n'_0, L}^<(E) + \Sigma_{n_0, n'_0, R}^<(E), \quad (27)$$

where the off-diagonal element of matrix, $\Sigma_{n_0, n'_0, \alpha}^<$, are zero and the diagonal ($n'_0 = n_0$) element of the lesser self-energy may be written as

$$\begin{aligned} \Sigma_{n_0, n_0, \alpha}^<(E) &= i\Gamma_{\alpha} \int d\varepsilon_{\alpha} f_{\alpha}(\varepsilon_{\alpha}) B_{n_0} \delta(E - \varepsilon_{\alpha} - (n_0 + \frac{1}{2})\hbar\omega) \\ &= i\Gamma_{\alpha} f_{\alpha}(\varepsilon) B_{n_0}, \end{aligned} \quad (28)$$

where $\varepsilon = E - n_0 + (\frac{1}{2})\hbar\omega$, $f_{\alpha}(\varepsilon_{\alpha})$ and $f_{\alpha}(\varepsilon)$ are the Fermi distribution functions of the left ($\alpha = L$) and right ($\alpha = R$) leads, which have different chemical potentials under a voltage bias and B_{n_0} is the Boltzmann factor for the oscillator state. Index n_0 determines the statistical occupation probability of the phonon state $|n_0\rangle$ at finite temperature and therefore the accessibility of particular conduction channels is determined by a weight factor of the Boltzmann distribution function.

Following equation (20), the formula for the current through each of the leads is written in terms of oscillator indices as

$$\begin{aligned} I_{\alpha} &= \frac{e}{2\pi\hbar} \sum_{n_0, n} \int \left\{ \Sigma_{n_0, n, \alpha}^<(E) (G_{n, n_0}^r(E) - G_{n, n_0}^a(E)) \right. \\ &\quad \left. + (\Sigma_{n_0, n, \alpha}^a(E) - \Sigma_{n_0, n, \alpha}^r(E)) G_{n, n_0}^<(E) \right\} dE \end{aligned} \quad (29)$$

With the help of equation (29), the net current through the dot and the leads with the oscillator on the dot is written as

$$\begin{aligned}
I &= \frac{I_L - I_R}{2} \\
&= \frac{e}{4\pi\hbar} \sum_{n_0, n} \int \left\{ (\Sigma_{n_0, n, L}^<(E) - \Sigma_{n_0, n, R}^<(E)) (G_{n, n_0}^r(E) - G_{n, n_0}^a(E)) \right. \\
&\quad \left. + [(\Sigma_{n_0, n, L}^a(E) - \Sigma_{n_0, n, L}^r(E)) - (\Sigma_{n_0, n, R}^a(E) - \Sigma_{n_0, n, R}^r(E))] G_{n, n_0}^<(E) \right\} dE.
\end{aligned} \tag{30}$$

The resulting expression for the net current is

$$I = \frac{e}{4\pi\hbar} \sum_{n_0, n} \int \left\{ (\Sigma_{n_0, n, L}^< - \Sigma_{n_0, n, R}^<)_{\alpha} [G_{n, n_0}^r(E) - G_{n, n_0}^a(E)] \right\} dE, \tag{31}$$

which is derived from equation (30) using the same damping factor for each lead ($\Gamma_L = \Gamma_R = \Gamma$).

For the present case of zero temperature the lesser self-energy may be recast in terms of the Heaviside step function $\theta(x)$ as

$$\Sigma_{n_0, n_0, \alpha}^< = i\Gamma_{\alpha} \theta(\epsilon_{F\alpha} - \epsilon) \delta_{n_0, 0}, \tag{32}$$

where $\epsilon_{F\alpha}$ is the Fermi energy on lead α and the Kronecker delta, $\delta_{n_0, 0}$, signifies that the nanomechanical oscillator is initially in its ground state, $n_0 = 0$.

Inserting this equation in the above equation, the result is

$$\begin{aligned}
I &= \frac{e}{2\pi\hbar} \int dE [T_0(E)] \\
&\quad \times [\theta(\epsilon_{FL} + \frac{1}{2}\hbar\omega - E) - \theta(\epsilon_{FR} + \frac{1}{2}\hbar\omega - E)] \tag{33}
\end{aligned}$$

where

$$T_0(E) = \frac{i\Gamma}{2} (G_{0,0}^r(E) - G_{0,0}^a(E)) = \Gamma [G_{0,0}^r(E) \Gamma G_{0,0}^a(E)]$$

Using the expression for the retarded and advanced Green's function, the expression for the net current becomes

$$\begin{aligned}
I &= \frac{e}{2\pi\hbar} \sum_n |\Phi_{0,n}|^2 \\
&\quad \times \int_{\epsilon_{FR} + \frac{1}{2}\hbar\omega}^{\epsilon_{FL} + \frac{1}{2}\hbar\omega} \frac{\Gamma^2 dE}{[E - \epsilon_0 - (n + \frac{1}{2})\hbar\omega + \Delta]^2 + \Gamma^2} \tag{34}
\end{aligned}$$

After performing the integral in the above expression, the final result is written as

$$\begin{aligned}
I &= \frac{e\Gamma}{2\pi\hbar} \sum_n |\Phi_{0,n}|^2 \left[\tan^{-1} \left(\frac{\epsilon_{FL} - \epsilon_0 - n\hbar\omega + \Delta}{\Gamma} \right) \right. \\
&\quad \left. - \tan^{-1} \left(\frac{\epsilon_{FR} - \epsilon_0 - n\hbar\omega + \Delta}{\Gamma} \right) \right] \tag{35}
\end{aligned}$$

The model represent the interplay between two physical time scales of the system, the oscillator frequency and the tunneling rate. This model also shows the very interesting interplay between two physical length scales of the system, zero point amplitude and zero point displacement, which actually affected by the weak and strong coupling dynamics.

The zero frequency shot-noise has been derived and applied successfully in many examples of the transport dynamics of nanoscopic systems^{17,24,26}. This is given as

$$S(0) = \frac{e^2}{\pi\hbar} \int \left\{ [f_L(\epsilon)(1 - f_L(\epsilon)) + f_R(\epsilon)(1 - f_R(\epsilon))] T_0(E) + [f_L(\epsilon) - f_R(\epsilon)]^2 (1 - T_0(E)) T_0(E) \right\} dE, \tag{36}$$

Using the values of transmission coefficients at zero temperature, the above expression can be simplified as

$$\begin{aligned}
S(0) &= \frac{e^2}{\pi\hbar} \int_{\epsilon_{FR} + \frac{1}{2}\hbar\omega}^{\epsilon_{FL} + \frac{1}{2}\hbar\omega} (1 - T_0(E)) T_0(E) dE \\
&= \frac{e^2}{\pi\hbar} \int_{\epsilon_{FR} + \frac{1}{2}\hbar\omega}^{\epsilon_{FL} + \frac{1}{2}\hbar\omega} \left\{ \sum_n \frac{|\Phi_{0,n}|^2 \Gamma^2}{[E - \epsilon_0 - (n + \frac{1}{2})\hbar\omega + \Delta]^2 + \Gamma^2} - \left(\sum_n \frac{|\Phi_{0,n}|^2 \Gamma^2}{[E - \epsilon_0 - (n + \frac{1}{2})\hbar\omega + \Delta]^2 + \Gamma^2} \right)^2 \right\} dE
\end{aligned} \tag{37}$$

After integrating the above expression, we arrive at the final result

$$S(0) = \frac{e^2\Gamma}{\pi\hbar} \left\{ \sum_n S_n(0) + \sum_{n>m} S_{n,m}(0) \right\}, \tag{38}$$

where $S_n(0)$ and $S_{n,m}(0)$ are defined as

$$\begin{aligned}
S_n(0) &= |\Phi_{0,n}|^2 \left\{ \left[\tan^{-1} \left(\frac{\epsilon_{FL} - \epsilon_0 - n\hbar\omega + \Delta}{\Gamma} \right) - \tan^{-1} \left(\frac{\epsilon_{FR} - \epsilon_0 - n\hbar\omega + \Delta}{\Gamma} \right) \right] \right. \\
&\quad + \frac{|\Phi_{0,n}|^2}{2} \left[\frac{\Gamma(\epsilon_{FL} - \epsilon_0 - n\hbar\omega + \Delta)}{(\epsilon_{FL} - \epsilon_0 - n\hbar\omega + \Delta)^2 + \Gamma^2} + \tan^{-1} \left(\frac{\epsilon_{FL} - \epsilon_0 - n\hbar\omega + \Delta}{\Gamma} \right) \right] \\
&\quad \left. - \frac{|\Phi_{0,n}|^2}{2} \left[\frac{\Gamma(\epsilon_{FR} - \epsilon_0 - n\hbar\omega + \Delta)}{(\epsilon_{FR} - \epsilon_0 - n\hbar\omega + \Delta)^2 + \Gamma^2} - \tan^{-1} \left(\frac{\epsilon_{FR} - \epsilon_0 - n\hbar\omega + \Delta}{\Gamma} \right) \right] \right\} \\
S_{n,m}(0) &= \frac{|\Phi_{0,n}|^2 |\Phi_{0,m}|^2 \Gamma^2}{i((n-m)\hbar\omega)((n-m)\hbar\omega + 2i\Gamma)} \left\{ \frac{1}{2} \ln \left[\frac{(\epsilon_{FL} - \epsilon_0 - n\hbar\omega + \Delta)^2 + \Gamma^2}{(\epsilon_{FR} - \epsilon_0 - n\hbar\omega + \Delta)^2 + \Gamma^2} \right] \right. \\
&\quad \left. + i \left(\tan^{-1} \left[\frac{\epsilon_{FL} - \epsilon_0 - n\hbar\omega + \Delta}{\Gamma} \right] - \tan^{-1} \left[\frac{\epsilon_{FR} - \epsilon_0 - n\hbar\omega + \Delta}{\Gamma} \right] \right) \right\} \\
&\quad + \frac{|\Phi_{0,n}|^2 |\Phi_{0,m}|^2 \Gamma^2}{i((m-n)\hbar\omega)((m-n)\hbar\omega + 2i\Gamma)} \left\{ \frac{1}{2} \ln \left[\frac{(\epsilon_{FL} - \epsilon_0 - m\hbar\omega + \Delta)^2 + \Gamma^2}{(\epsilon_{FR} - \epsilon_0 - m\hbar\omega + \Delta)^2 + \Gamma^2} \right] \right. \\
&\quad \left. + i \left(\tan^{-1} \left[\frac{\epsilon_{FL} - \epsilon_0 - m\hbar\omega + \Delta}{\Gamma} \right] - \tan^{-1} \left[\frac{\epsilon_{FR} - \epsilon_0 - m\hbar\omega + \Delta}{\Gamma} \right] \right) \right\}
\end{aligned}$$

The corresponding Fano factor can be calculated from the zero frequency noise and the net current flowing through the system, which is defined as

$$F = \frac{S(0)}{2eI} \tag{39}$$

III. DISCUSSION OF RESULTS

The current-voltage (I-V) characteristics, shot noise spectrum and the corresponding Fano factor of a resonant tunnel junction coupled to a nanomechanical oscillator are shown graphically for different values of coupling strength, using the same parameters as: the single energy level of the dot $\epsilon_0 = 0.5$, the characteristic frequency of

the oscillator $\hbar\omega = 0.1$, the damping factor $\Gamma = 0.1\hbar\omega$ and the chemical potentials $0 \leq \epsilon_{FL} \leq 1$ and $\epsilon_{FR} = 0$. These are chosen to illustrate the physics of such systems rather than to represent a specific implementation. The oscillator induced resonance effects are clearly visible in the numerical results. It must be noted that we have obtained these results in the regime of strong and zero or weak coupling of the oscillator with the electrons on the dot. The coupling between the leads and the dot is considered to be symmetric and we assume that the electrons in the leads are at zero temperature and have constant density of states. With increasing coupling strength, the number of additional steps also increases while for zero or weak coupling we find only the basic resonance step. This confirms the effect of the coupling between the electrons on the dot and the single oscillator mode where higher energy electrons are able to drop to the dot energy by

creation of phonons.

Closer analytical examination of the expression for the current and shot noise (35 & 38) shows that the main resonance steps occur when the applied voltage, ϵ_{FL} is equal to the energy eigenvalues of the coupled dot electron and the nanomechanical oscillator. The main step ($n = 0$) is given by the Lorentzian form with its center at the $\epsilon_{FL} = \epsilon_0 - \Delta$, known as a Breit-Wigner resonance. The additional steps due to the emission of phonons can be seen on the positive energy side with $\epsilon_{FL} = \epsilon_0 - \Delta + n\hbar\omega$ where ω is the characteristic frequency of the nanomechanical oscillator. We have shown the I-V characteris-

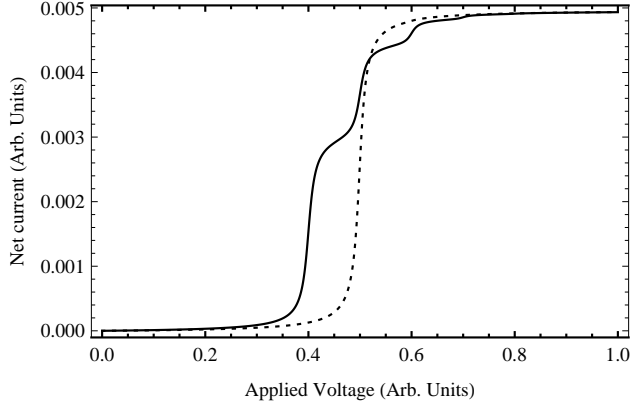


FIG. 1: Current-voltage characteristics (dimensionless) as a function of applied voltage ϵ_{FL} (in arbitrary units), coupling strength $\eta = 0.1\hbar\omega$ (dotted line) and $1\hbar\omega$ (solid line). Gate voltage $\epsilon_0 = 0.5$, oscillator energy $\hbar\omega = 0.1$ and self-energy $\Gamma = 0.1\hbar\omega$.

tics of the NEMS device against applied bias for different values of the coupling strength in Fig. 1. The main resonance step is the elastic or zero phonon transition. The amplitude of the additional steps is much smaller than the basic resonance step. The electrons that tunnel onto the dot can only excite the oscillator mode as at zero temperature there are no phonons available to be absorbed. Moreover, we have seen that with increasing coupling strength, the number and intensity of the additional steps increases but their intensity always remains much smaller than the main step. The steps in the current characteristics vanish if the upper electrochemical potential is smaller than the dot energy plus the oscillator energy.

Next, we have shown the shot noise as a function of applied bias in Fig. 2, which exhibits the single step in the presence of weak or zero electron-oscillator coupling while the number of additional steps increases with increasing coupling strength. Obviously, the shape of the shot noise curve is similar to that of the net current, as shown in Fig. 1. The only difference is associated with their behavior above the resonance point, where the noise power for the strong coupling case can exceed the shot noise for the zero phonon case. We also show the differential shot noise against applied bias for different

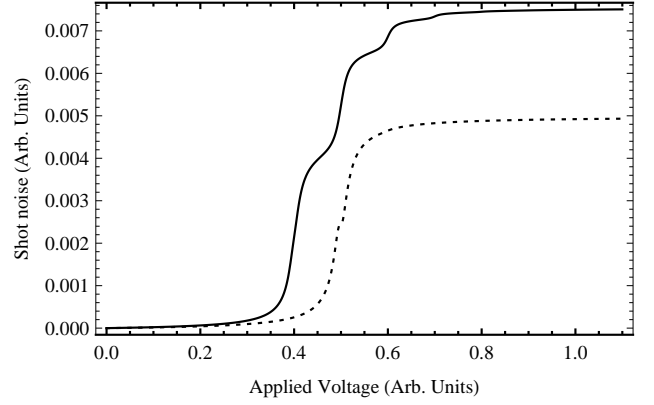


FIG. 2: Shot noise (dimensionless) as a function of applied voltage ϵ_{FL} (in arbitrary units), with gate voltage $\epsilon_0 = 0.5$, oscillator energy $\hbar\omega = 0.1$, self-energy $\Gamma = 0.1\hbar\omega$, and coupling strength $\eta = 0.1\hbar\omega$ (dotted line) and $1\hbar\omega$ (solid line).

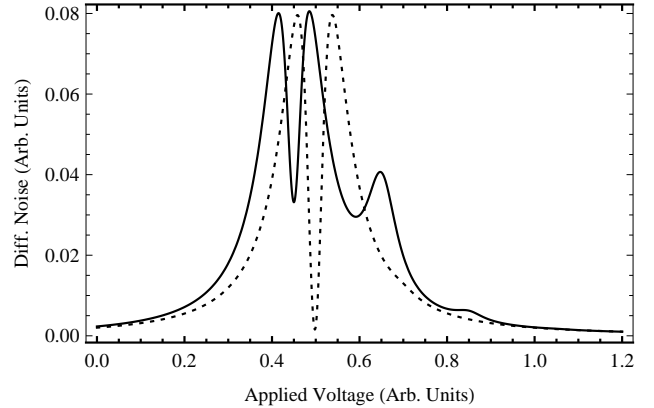


FIG. 3: Differential shot noise (dimensionless) as a function of applied voltage ϵ_{FL} (in arbitrary units) with gate voltage $\epsilon_0 = 0.5$, oscillator energy $\hbar\omega = 0.2$, self-energy $\Gamma = 0.2\hbar\omega$ and coupling strength $\eta = 0.1\hbar\omega$ (dotted line) and $\eta = 0.5\hbar\omega$ (solid line).

values of the coupling strength (in Fig. 3). In the absence of phonons, when the transport is coherent, the shot noise spectrum exhibits two peaks separated by an antiresonance and located symmetrically around the position where the current step associated with the single level of the dot is located. The origin of such an antiresonance in the noise spectrum is associated with the fact that no noise is generated when the transmission via the dot state is perfect, $T = 1$ or zero. Due to the presence of the nanomechanical oscillator, the main resonance peaks are shifted by Δ . Meanwhile, the sharp peaks are now accompanied by a set of additional peaks. We note that the separation between the differential shot noise peaks is set by the frequency of the oscillator. This phenomenon can be explained on the basis of phonon emission during electron-phonon coupling, indicating that a new channel

has opened and contributes to the resonant tunneling process.

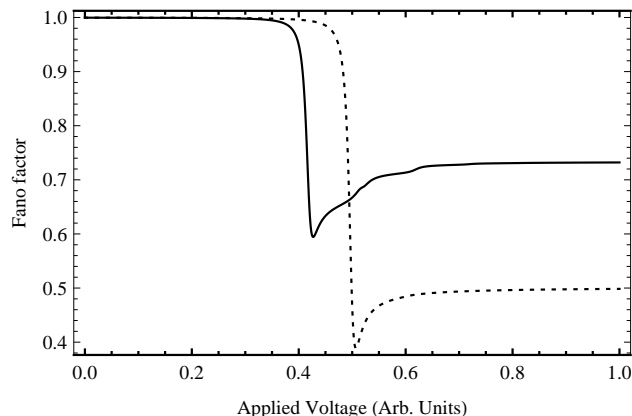


FIG. 4: Fano factor as a function of applied voltage ϵ_{FL} (in arbitrary units) with gate voltage $\epsilon_0=0.5$, oscillator energy $\hbar\omega = 0.1$, self-energy $\Gamma = 0.1\hbar\omega$ and coupling strength $\eta = 0.1\hbar\omega$ (dotted line) and $\eta = 1\hbar\omega$ (solid line).

Finally, we have shown the Fano factor against applied bias for different values of the coupling strength. Information about the statistical properties of the electrons is included in the Fano factor, which is plotted in Fig. 4. Since in our model all the interactions between the current carriers are neglected, such electron correlations are associated only with the Coulomb blockade. This principle is related to the fact that one electron feels the presence of the others, since it cannot occupy

the state on the dot already occupied by the electron. The crossover in the shot noise power from Poissonian ($F=1$) to sub-Poissonian ($F<1$) is always observed after the first step in the current voltage dependence. This implies that electrons tunnel in a correlated way in the NEMS device. The most important result is the significant enhancement of the Fano factor due to the phonon effects, observed for $\epsilon_{FL} > \epsilon_0 - \Delta + n\hbar\omega$, where the multi-channel process reduces electron correlations compared with the single channel case. Moreover, the shift Δ can also be easily recognized in Fig. 4.

IV. SUMMARY

In this work, we analyzed the current noise characteristics of a resonant tunnel junction coupled to a nanomechanical oscillator by using the non-equilibrium Green's function approach without treating the electron-phonon coupling as a perturbation. We have derived analytical expressions for the net current flowing through the system and for the shot noise. This enables us to see the effects of the coupling of the electrons to the oscillator on the dot and the tunneling rate of electrons. We show the numerical results for very weak and strong coupling strength. We have found additional steps or peaks due to coupling of single phonon mode which are absent for very weak or no coupling strength. We also discuss the corresponding Fano factor as a function of applied bias which shows thermal or poissonian behavior to non-thermal or sub-poissonian behavior.

* Permanent address: Department of Physics, University of Sargodha, Sargodha, Pakistan; E-Mail: m.tahir@uos.edu.pk; M.Tahir would like to acknowledge the support of the Pakistan Higher Education Commission (HEC).

† E-Mail: a.mackinnon@imperial.ac.uk

¹ M. D. La Haye, O. Buu, B. Camarota and K. C. Schwab, *Science* **304**, 74 (2004).; K. C. Schwab and M. L. Roukes, *Phys. Today* **58**, 36 (2005).

² A. Naik, O. Buu, M. D. La Haye, A. D. Armour, A. A. Clerk, M. P. Blencowe and K. C. Schwab, *Nature (London)* **443**, 193 (2006).

³ R. G. Knobel and A. N. Cleland, *Nature* **424**, 291 (2003).

⁴ M. Poggio, M. P. Jura, C. L. Degen, M. A. Topinka, H. J. Mamin, D. Goldhaber-Gordon and D. Rugar, *Nature Phys.* **4**, 635 (2008).

⁵ H. Park, J. Park, A. K. L. Lim, E. H. Anderson, A. Paul Alivisatos, and P. L. McEuen *Nature (London)* **407**, 57 (2000).

⁶ A. Schliesser, O. Arcizet, R. Rivière, G. Anetsberger and T. J. Kippenberg, *Nature Phys.* **5**, 509 (2009).

⁷ K. L. Ekinci and M. L. Roukes, *Review of Scientific Instruments* **76**, 061101 (2005).; K. L. Ekinci, *Small* **1**, No. 8-9, 786-797 (2005); M. L. Roukes, *Technical Digest of*

the 2000 Solid State Sensor and Actuator Workshop; "Nanoelectromechanical Systems"; H. G. Craighead, *Science* **290**, 1532 (2000).; P. Kim and C. M. Lieber, *Science* **126**, 2148 (1999).

⁸ S. D. Bennett and A.A. Clerk, *Phys. Rev. B* **78**, 165328 (2008).; S. Akita, Y. Nakayama, S. Mizooka, Y. Takano, T. Okawa, Y. Miyatake, S. Yamanaka, M. Tsuji and T. Nosaka, *Appl. Phys. Lett.* **79**, 1691 (2001).; A. M. Fenimore, T. D. Yuzvinsky, W. Q. Han, M. S. Fuhrer, J. Cummings and A. Zettl, *Nature* **424**, 408 (2003).

⁹ J. Kinaret, T. Nord and S. Viefers, *Appl. Phys. Lett.* **82**, 1287 (2003).; C.-H. Ke and H. D. Espinosa, *Appl. Phys. Lett.* **85**, 681 (2004).; V. Sazonova, Y. Yaish, H. Üstünel, D. Roundy, T. Arias and P. McEuen, *Nature* **431**, 284 (2004).

¹⁰ M. P. Blencowe, *Phys. Rep.* **395**, 159 (2004).; A. N. Cleland, *Foundations of Nanomechanics*, 2003 (Berlin: Springer).

¹¹ J. Repp, G. Meyer, S. M. Stojković, A. Gourdon and C. Joachim, *Phys. Rev. Lett.* **94**, 026803 (2005).

¹² J. Repp, G. Meyer, S. Paavilainen, F. E. Olsson and M. Persson, *Phys. Rev. Lett.* **95**, 225503 (2005).

¹³ X. H. Qiu, G. V. Nazin and W. Ho, *Phys. Rev. Lett.* **92**, 206102 (2004).

- ¹⁴ S. W. Wu, G. V. Nazin, X. Chen, X. H. Qiu and W. Ho, Phys. Rev. Lett. **93**, 236802 (2004).
- ¹⁵ A. D. Armour, Phys. Rev. B **70**, 165315 (2004).
- ¹⁶ N. M. Chtchelkatchev, W. Belzig and C. Bruder, Phys. Rev. B **70**, 193305 (2004).
- ¹⁷ V. Nam Do, P. Dollfus and V. Lien Nguyen, Appl. Phys. Lett. **91**, 022104 (2007).
- ¹⁸ A. A. Clerk and S. M. Girvin, Phys. Rev. B **70**, 121303(R) (2004).
- ¹⁹ D. Mozyrsky, I. Martin and M. B. Hastings, Phys. Rev. Lett. **92**, 018303 (2004).
- ²⁰ Bing Dong, H.L. Cui, X.L. Lei and Norman J.M. Horing, Phys. Rev. B **71**, 045331 (2005).
- ²¹ L. V. Keldysh, Zh. Eksp. Teor. Fiz. **47**, 1515 (1965) [Sov. Phys. JETP **20**, 1018 (1965)].
- ²² H. Haug and A. P. Jauho, Quantum Kinetics in Transport and Optics of Semiconductors, Springer Solid-State Sciences Vol. 123 (Springer, New York, 1996).
- ²³ D. K. Ferry and S. M. Goodnick, Transport in nanostructure, Cambridge University press, 2001.; S. Datta, J. Phys.: Condens. Matter **2**, 8023 (1990); R. Lake and S. Datta, Phys. Rev. B **45**, 6670 (1992); **46**, 4757 (1992).
- ²⁴ J. -X. Zhu and A. V. Balatsky, Phys. Rev. B **67**, 165326 (2003).
- ²⁵ M. Tahir and A. MacKinnon, Phys. Rev. B **77**, 224305 (2008).
- ²⁶ Michael Galperin, Abraham Nitzan and Mark A. Ratner, Phys. Rev. B **74**, 075326 (2006).
- ²⁷ D. A. Ryndyk, R. Gutiérrez, B. Song and G. Cuniberti, Springer Series in Chemical Physics, Volume **3**, pages 213-235 (2009).
- ²⁸ Michael Galperin, Mark A. Ratner, Abraham Nitzan and Alessandro Troisi, Science **319**, 1056 (2008).
- ²⁹ A. Shimizu and M. Ueda, Phys. Rev. Lett. **69**, 1403 (1992).
- ³⁰ O. L. Bo and Yu. Galperin, Phys. Rev. B **55**, 1696 (1997) ; Y.-C. Chen and M. Di Ventra, Phys. Rev. Lett. **95**, 166802 (2005).
- ³¹ N. Nishiguchi, Phys. Rev. Lett. **89**, 066802 (2002).
- ³² A. Yu. Smirnov, L. G. Mourokh and N. J. M. Horing, Phys. Rev. B **67**, 115312 (2003).
- ³³ J. Wabnig, D. V. Khomitsky, J. Rammer and A. L. Shelankov, Phys. Rev. B **72**, 165347 (2005).
- ³⁴ T. Novotný, A. Donarini, C. Flindt and A.-P. Jauho, Phys. Rev. Lett. **92**, 248302 (2004).; C. Flindt, T. Novotný and A.-P. Jauho, Phys. Rev. B **70**, 205334 (2004).
- ³⁵ D. Mozyrsky and I. Martin, Phys. Rev. Lett. **89**, 018301 (2002).
- ³⁶ I. S. Gradshteyn and I. M. Ryzhik, Tables of Integrals, Series and Products Academic, New York, (1980), P. 837.
- ³⁷ Ned S. Wingreen, Karsten W. Jacobsen and John W. Wilkins, Phys. Rev. B **40**, 11834 (1989).
- ³⁸ A. P. Jauho, N. S. Wingreen and Y. Meir, Phys. Rev. B **50**, 5528 (1994).
- ³⁹ V. Moldoveanu, V. Gudmundsson and A. Manolescu, Phys. Rev. B **76**, 085330 (2007).; J. Maciejko, J. Wang and H. Guo, Phys. Rev. B **74**, 085324 (2006).; Y. Wei and J. Wang, Phys. Rev. B **79**, 195315 (2009).; P. Myöhänen, A. Stan, G. Stefanucci and R. van Leeuwen, Phys. Rev. B **80**, 115107 (2009).; A. R. Hernández, F. A. Pinheiro, C. H. Lewenkopf and E.R. Mucciolo, Phys. Rev. B **80**, 115311 (2009).
- ⁴⁰ J. Maciejko, J. Wang and H. Guo, Phys. Rev. B **74**, 085324 (2006).